Science Advances
AAAS

Supplementary Materials for

A universal bacteriophage T4 nanoparticle platform to design multiplex SARS-CoV-2 vaccine candidates by CRISPR engineering

Jingen Zhu, Neeti Ananthaswamy, Swati Jain, Himanshu Batra, Wei-Chun Tang, Douglass A. Lewry, Michael L. Richards, Sunil A. David, Paul B. Kilgore, Jian Sha, Aleksandra Drelich, Chien-Te K. Tseng*, Ashok K. Chopra*, Venigalla B. Rao*

*Corresponding author. Email: rao@cua.edu (V.B.R.); sktseng@utmb.edu (C.-T.K.T.); achopra@utmb.edu (A.K.C.)

Published 8 September 2021, *Sci. Adv.* **7**, eabh1547 (2021)
DOI: 10.1126/sciadv.abh1547

The PDF file includes:

Other Supplementary Material for this manuscript includes the following:

Supplementary Materials

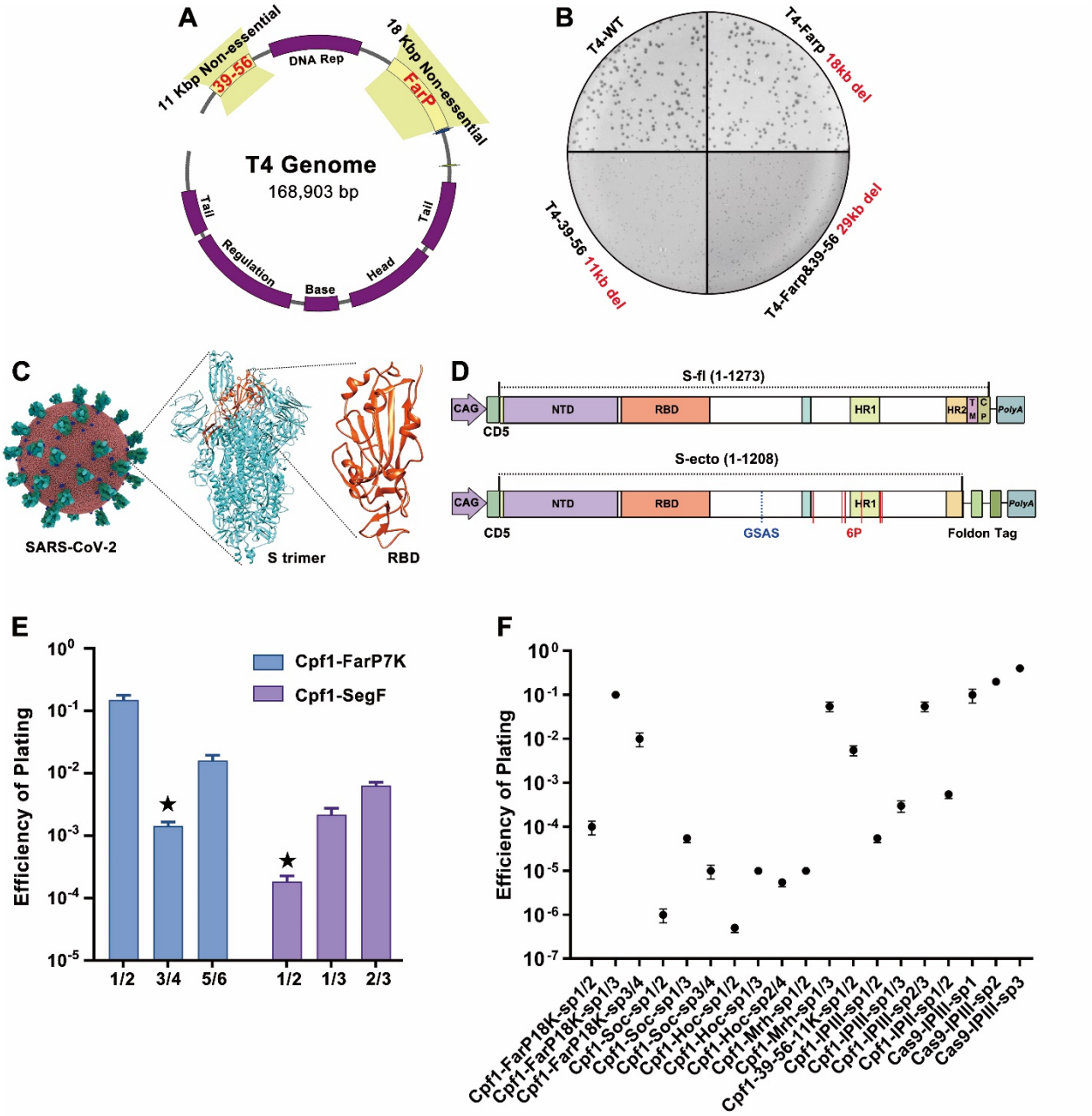

Figure S1. CRISPR engineering of non-essential T4 genome. (**A**) Schematic showing the 18-kb nonessential segment FarP and 11-kb nonessential segment 39-56 on T4 genome. (**B**) Plaque size of wild-type (WT), T4-*FarP 18-kb del.*, T4-*39-56 11-kb del.*, and T4-*FarP&39-56 29-kb del.* phages. Note the small size of T4-*39-56 11-kb del.* and T4-*FarP&39-56 29-kb del.* plaques. (**C**) Structural models of SARS-CoV-2 virus, spike trimer, and receptor binding domain (RBD). (**D**) Schematics of S-full length (S-fl) and S -ectodomain (S-ecto) expression cassettes used for insertion into T4 genome. (**E**) Efficiency of plating of three sets of Cpf1-FarP7K spacers and three sets of Cpf1-SegF spacers. (**F**) Efficiency of plating of various spacers used for T4 genome engineering in this study.

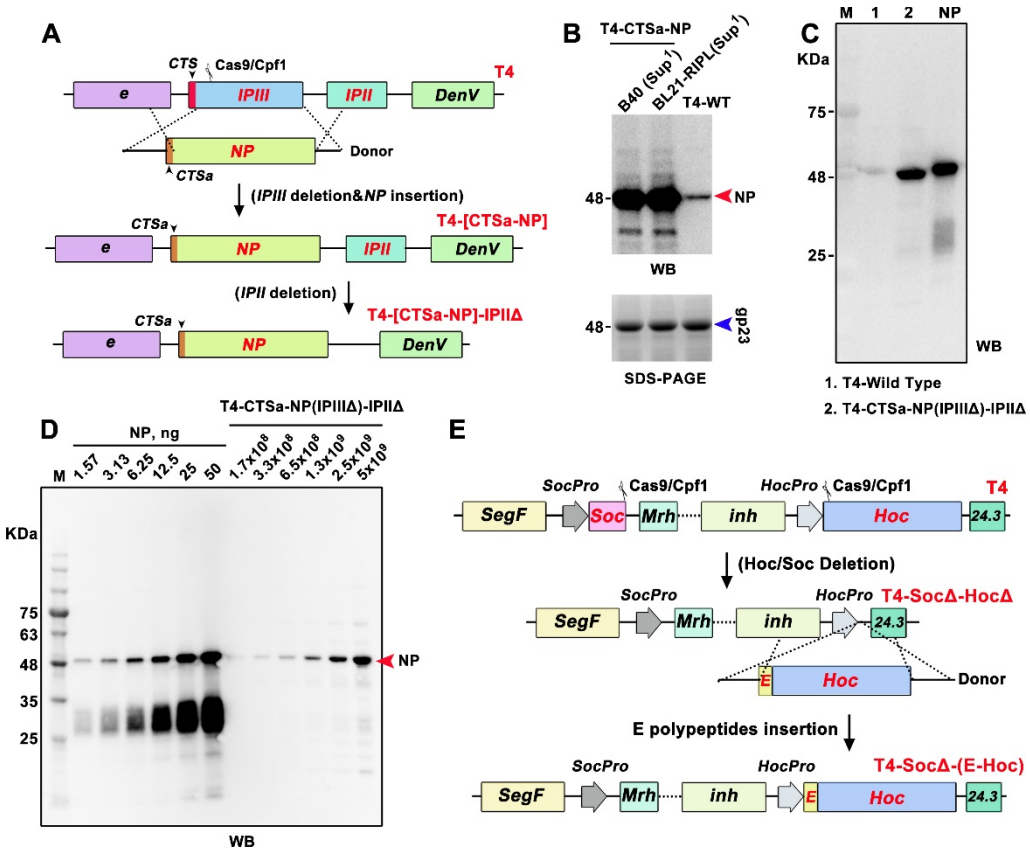

Figure S2. Engineering of NP encapsidation and Ee epitope display. (**A**) Schematic showing the construction of T4-IPIIIΔ-IPIIΔ-CTSam-NP phage. (**B**) Western Blot (WB) showing NP expression and encapsidation in *E. coli* B40 (*Sup*^{1}) and BL21-RIPL (*Sup*^{1}) infected with T4-CTSa-NP phage. (**C**) A second NP-specific monoclonal antibody was used to confirm the encapsidation of NP in the T4-CTSa-NP phage. (**D**) Quantification of the copy number of T4-encapsidated NP protein molecules by WB using commercial NP standard (Sino Biological). (**E**) Schematic showing the construction of T4-SocΔ-HocΔ and T4-SocΔ-(E epitope-Hoc) phages.

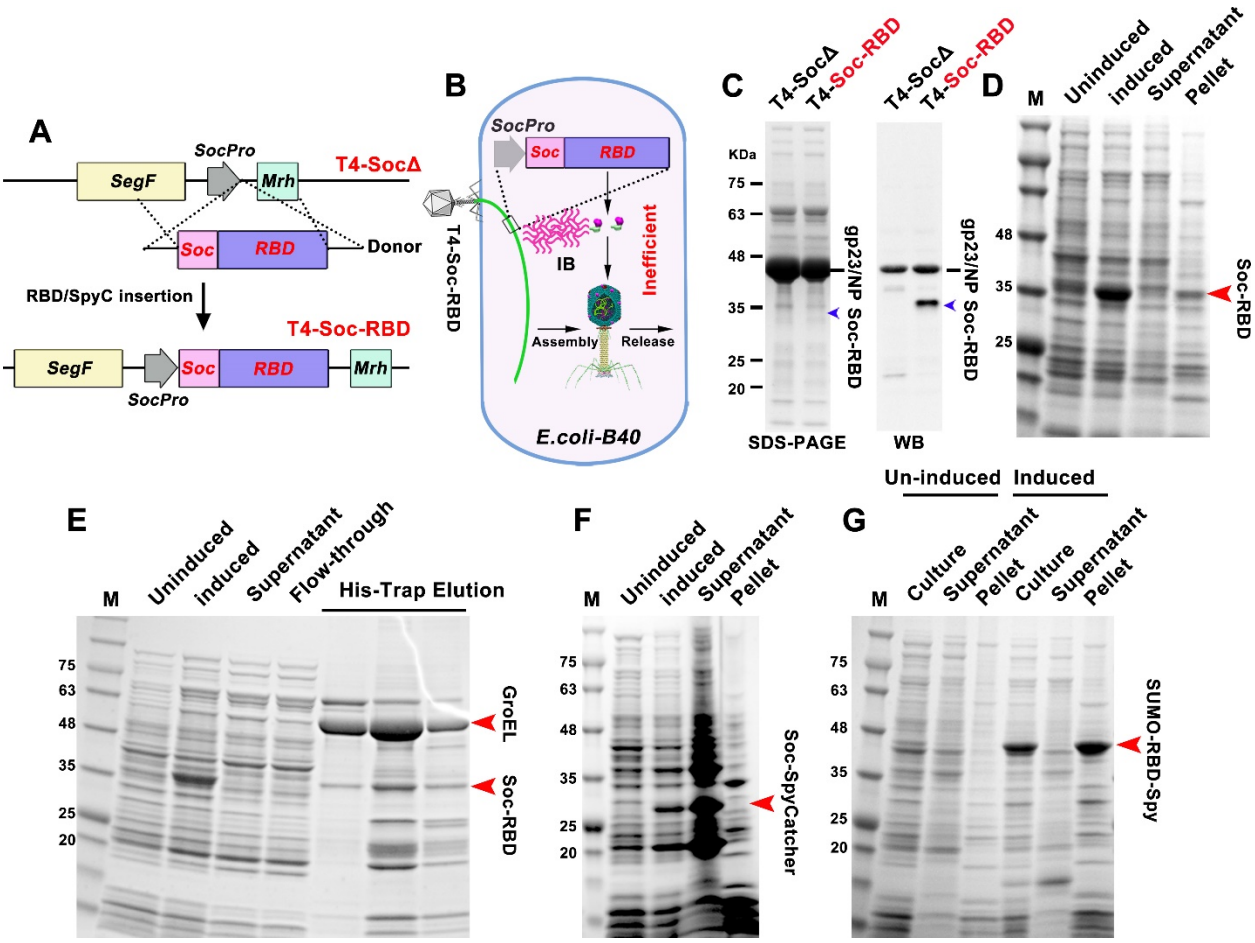

Figure S3. Engineering and solubility analysis of Soc-RBD, SUMO-RBD-SpyTag, and Soc-SpyCatcher constructs. (**A**) Schematic showing the insertion of Soc-RBD gene into phage genome at the Soc deletion site. (**B** and **C**) Schematic (**B**) and SDS-PAGE/WB (**C**) showing inefficient *in vivo* display of *E. coli*-expressed sRBD on T4 phage. IB, inclusion body. No significant Soc-RBD band was observed by SDS-PAGE but it could be detected by WB. Anti-RBD polyclonal antibody (Sino Biological) used here non-specifically recognized T4 gp23. (**D**) Solubility analysis of Soc-RBD. The presence of Soc-RBD in the pellet and absence in the supernatant of *E. coli* lysate indicates insolubility. (**E**) Very little soluble Soc-RBD was recovered after concentration of the any soluble Soc-RBD by purification on a HisTrap Ni^{2+} affinity column. No significant Soc-RBD was detected in supernatant and flow-through, but a small amount of Soc-RBD was co-eluted with *E. coli* GroEL chaperone. (**F**) Solubility analysis of Soc-SpyCatcher. Soc-SpyCatcher expression was driven by the phage T7 promoter. Most of the expressed Soc-SpyCatcher protein remained in the supernatant indicating its high solubility. (**G**) Solubility analysis of SUMO-RBD-SpyTag. SUMO-RBD-SpyTag is insoluble, similar to Soc-RBD.

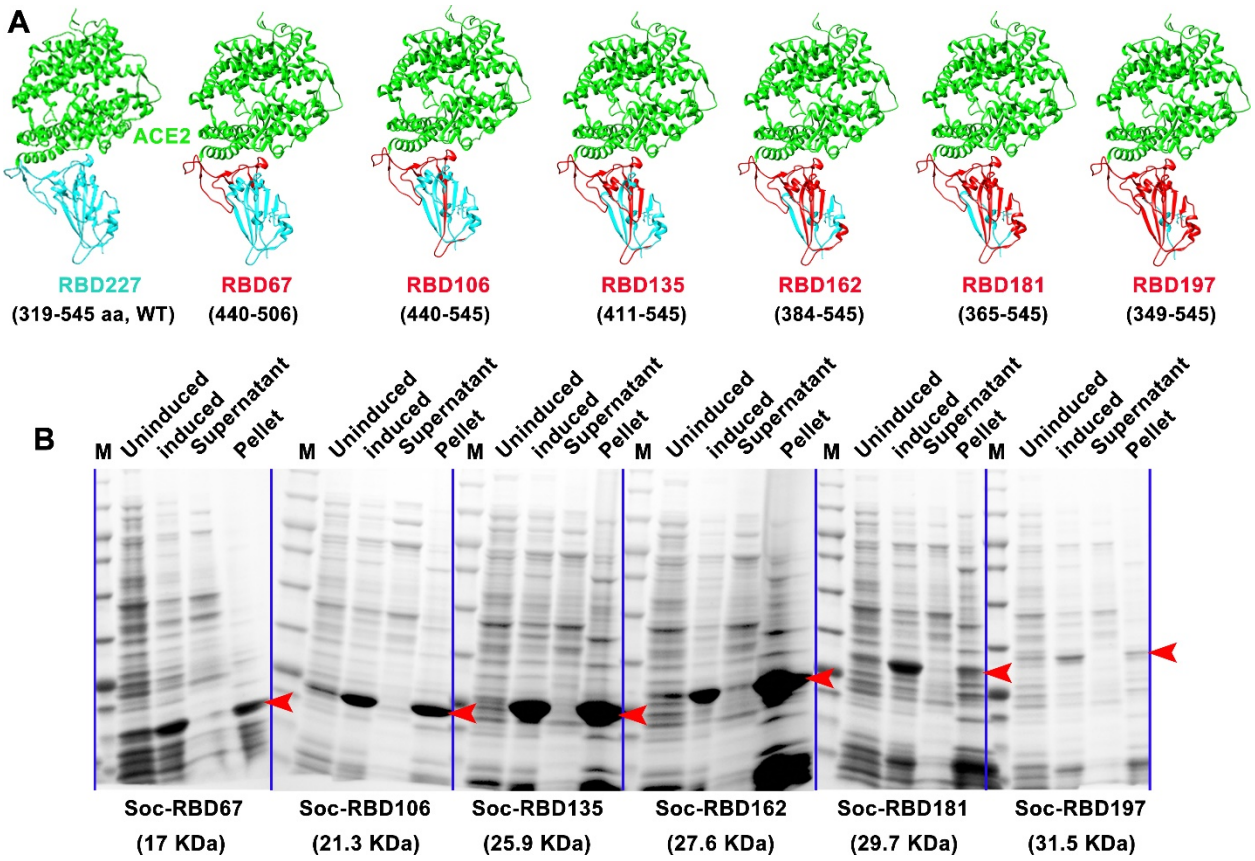

Figure S4. Construction and screening of various truncated SARS-CoV-2 RBDs. (**A**) Structural models of recombinant WT RBD and various truncated RBDs bound to human ACE2. ACE2 is shown in green. The truncated RBD clones are shown in red and the WT RBD and deleted regions are shown in cyan. The Protein Data Bank (PDB) code for the SARS-CoV-2 RBD–ACE2 complex is 6M0J (*39*). The truncated RBDs were generated using Chimera software. (**B**) Solubility analysis of Soc-fused truncated RBDs after cloning and expression in *E. coli* under the control of the phage T7 promoter. After lysis of *E. coli* and centrifugation, the supernatant and pellet were analyzed by SDS-PAGE. The presence of Soc-truncated RBDs in the pellet and their absence in the supernatant demonstrated insolubility. The red arrowheads indicate the band positions of various Soc-truncated RBDs.

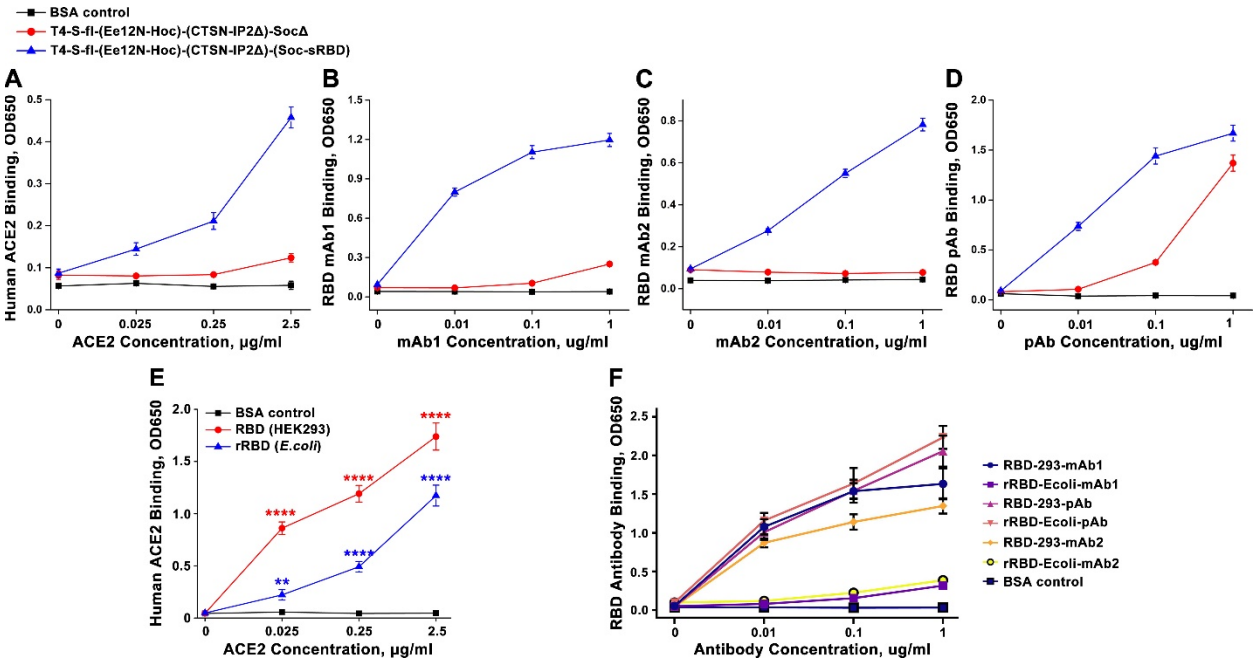

Figure S5. Comparison of ACE2 and RBD-antibody binding of T4-sRBD, *E.coli*-rRBD, and HEK293-RBD. (A to **D**) ACE2 and a panel of RBD-specific antibodies used for quantification by ELISA. (**E**) Comparison of binding of *E. coli*-produced rRBD to human ACE2 with the HEK293-produced RBD. **P < 0.01 and ****P < 0.0001. ns, no significance, P > 0.05. (**F**) Comparison of *E. coli*-produced rRBD and human HEK293-produced RBD using a panel of RBD-specific mAbs and pAbs. The HEK293-RBD showed much greater binding to mAb1 and mAb2 than the *E. coli* rRBD, while binding to pAbs was similar.

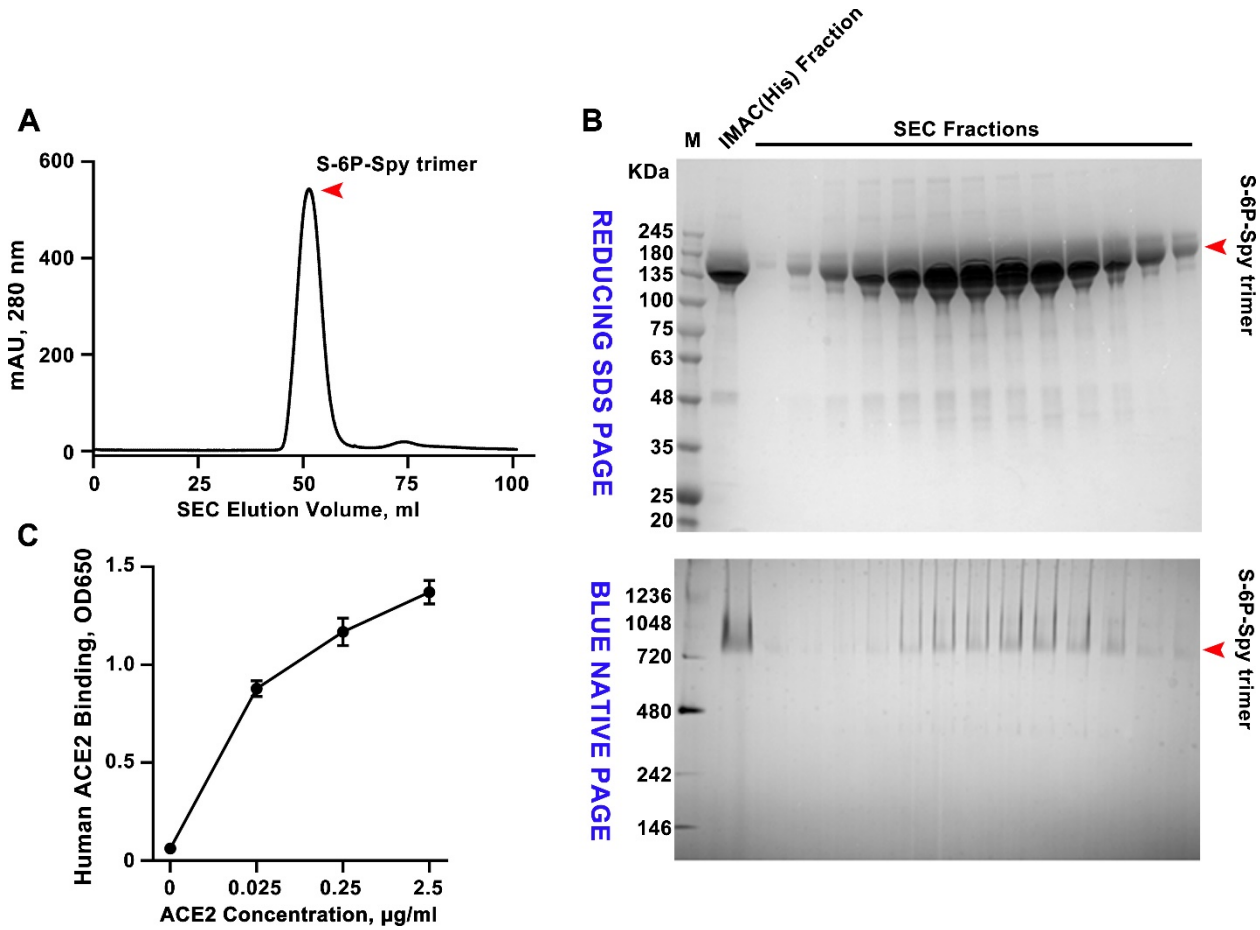

Figure S6. Purification and characterization of S-ecto-SpyTag trimers from ExpiCHO cells. (**A**) Size-exclusion chromatography (SEC) elution profile of S-ecto-SpyTag (S-ecto-Spy) trimers. HisTrap affinity purified S-ecto-spy protein from 250 ml of transfected ExpiCHO cells was loaded on Superdex 200 prep-grade SEC column. S-trimers yield was ~50 mg per 1 L culture. (**B**) Reducing SDS-PAGE (top) and BLUE NATIVE-PAGE (bottom) patterns of SEC-purified trimer fractions. The molecular weight standards (M) in kDa are shown on the left of the gels. IMAC (Immobilized Metal Affinity Chromatography, His) fraction is the material from affinity purification of culture supernatant on a HisTrap column, which was then loaded on the SEC column. (**C**) ELISA analysis showing the binding of purified S-trimers to human ACE2 at various ACE2 concentrations.

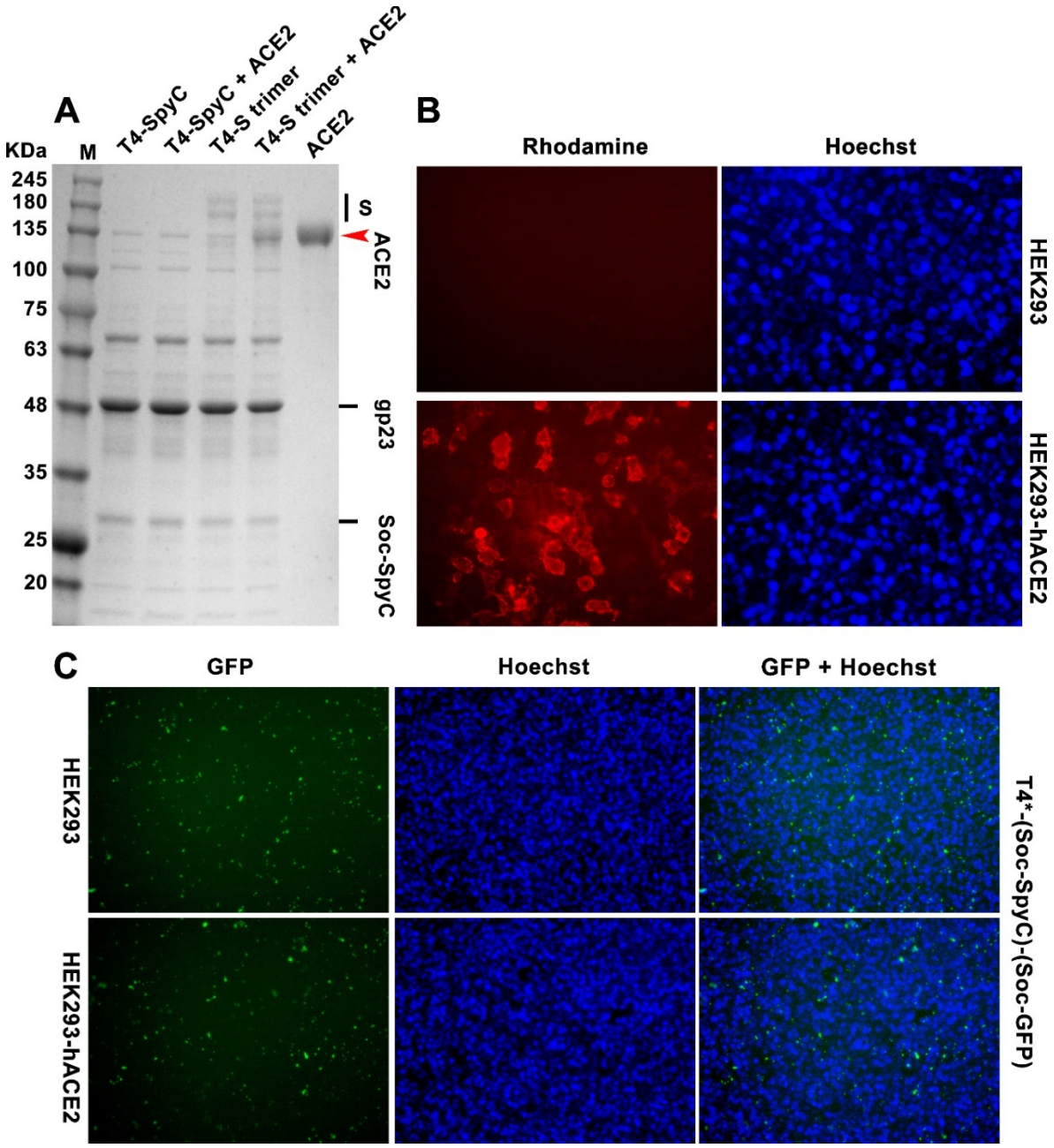

Figure S7. Binding of T4 phage-decorated S-trimers to ACE2-expressing HEK293 cells. (**A**) Co-sedimentation assay showing the capture of ACE2 by T4 phage-decorated S trimers. T4-S-trimer particles and ACE2 were incubated at an equimolar ratio for 1 hr at 4°C, followed by high-speed centrifugation. After two washes, the pellet was re-suspended in buffer and SDS-PAGE was performed. The presence of ACE2 in the pellet was found with these phage particles but not with the control phage lacking S-trimers. (**B**) Immunofluorescence assay showing expression of ACE2 on 293 cells. Two days after ACE2 plasmid transfection, HEK293 cells were incubated with RBD, followed by anti-RBD antibody and Rhodamine-conjugated second antibody. (**C**) Lack of binding of T4-GFP control phage (without S-trimers) to ACE2-293 cells. No difference in fluorescence was observed. The nuclei were stained with Hoechst. T4* indicates T4-(S-ecto) RBD-NP-Ee-SocΔ.

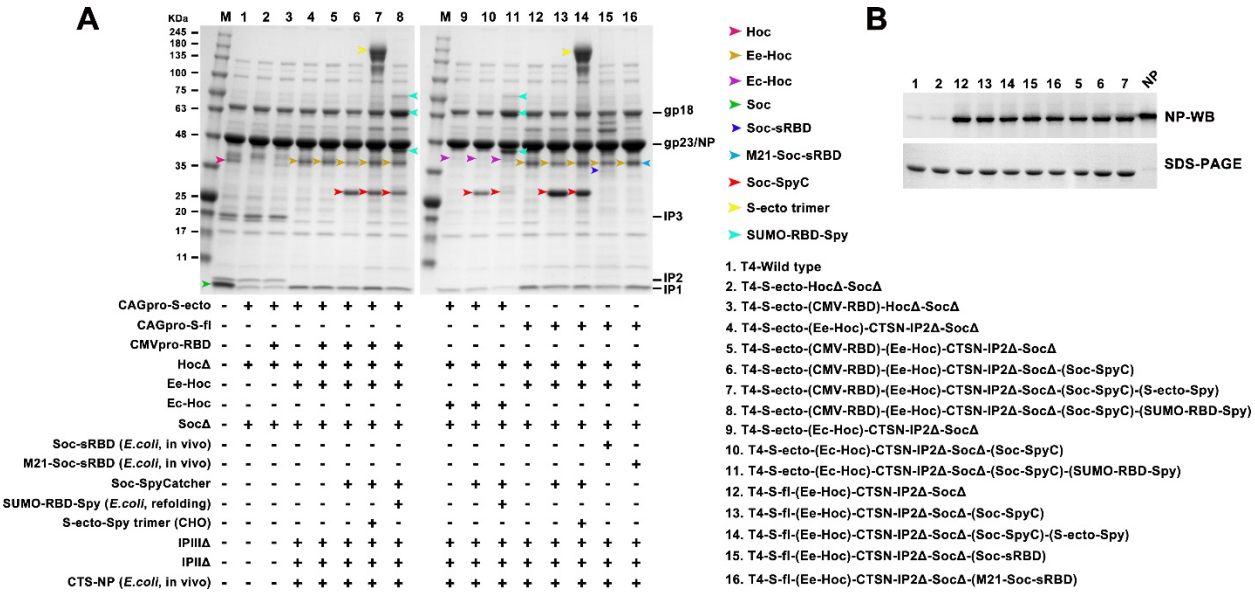

Figure S8. A pipeline of SARS-CoV-2 vaccine candidates generated by sequential CRISPR engineering. (**A**) One example of sequential phage CRISPR engineering for creating the T4-SARS-CoV-2 nanovaccine. Numerous CoV-2 components, including CAGpromoter-S-ecto insertion, CAGpromoter-S-fl insertion, CMVpromoter-RBD insertion, Hoc deletion, Ee-Hoc insertion, Ec-Hoc insertion, Soc deletion, Soc-sRBD display, M21-Soc-sRBD display, Soc-SpyCatcher display, refolding SUMO-RBD-Spy display, S-trimer display, IPIII deletion, IPII deletion, and NP encapsidation, were permutated and combined as needed. The resultant SARS-CoV-2 vaccine candidates were characterized by PCR, DNA sequencing and/or SDS-PAGE, and some of these were then tested in a mouse study. M21 indicates a potential T cell 21 aa epitope (SYFIASFRLFARTRSMWSFNP) from SARS-CoV-2 membrane protein. (**B**) WB showing NP protein encapsidation in the phages containing CTSam-NP insertion at IPIII deletion site.

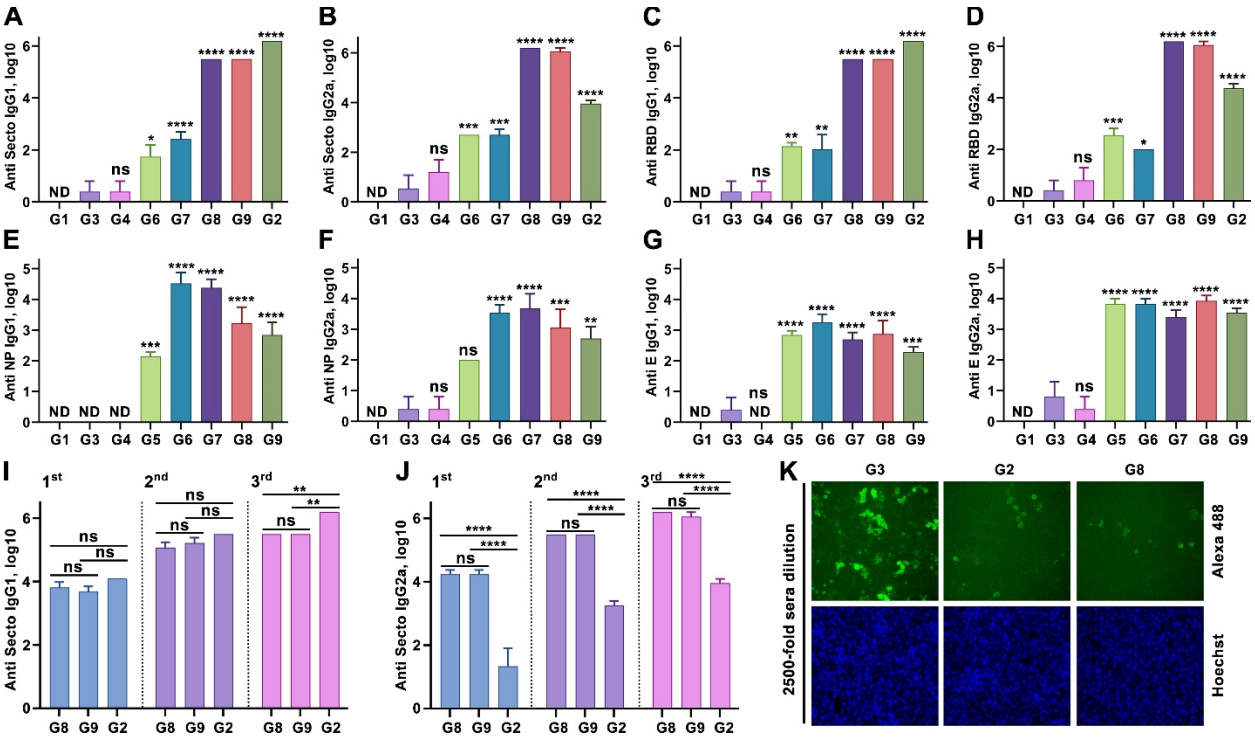

Figure S9. Serum antibody responses in various T4-SARS-CoV-2 immunized mice. (**A** and **B**) Anti-S-ecto IgG1 (**A**) and IgG2a (**B**) antibody titers in the boost-2 sera (week 8 bleeding) from various groups. (**C** and **D**) Anti-RBD IgG1 (**C**) and IgG2a (**D**) antibody titers in the boost-2 sera. (**E** and **F**) Anti-NP IgG1 (**E**) and IgG2a (**F**) antibody titers in the boost-2 sera. (**G** and **H**) Anti-E IgG1 (**G**) and IgG2a (**H**) antibody titers in the boost-2 sera. *P < 0.05, **P < 0.01, ***P < 0.001, and ****P < 0.0001, compared with phage control group G3. ns, no significance, P > 0.05. ND, not detected. (**I** and **J**) Anti-S-ecto IgG1 (**I**) and IgG2a (**J**) antibody titers in the sera from S-trimer & Alhydrogel (G2) group and T4-S-trimer (G8 and G9) groups at 2 weeks (prime), 5 weeks (boost-1), and 8 weeks (boost-2). **P < 0.01 and ****P < 0.01. (**K**) Blocking of native RBD protein binding to HEK293-ACE2 by 2500-fold diluted sera. Sera from the phage control group (G3), S-trimers-Alhydrogel group (G2), and T4-S-trimers group (G8) were compared. The RBD binding to ACE2 was detected by Alexa 488 conjugated secondary antibody.

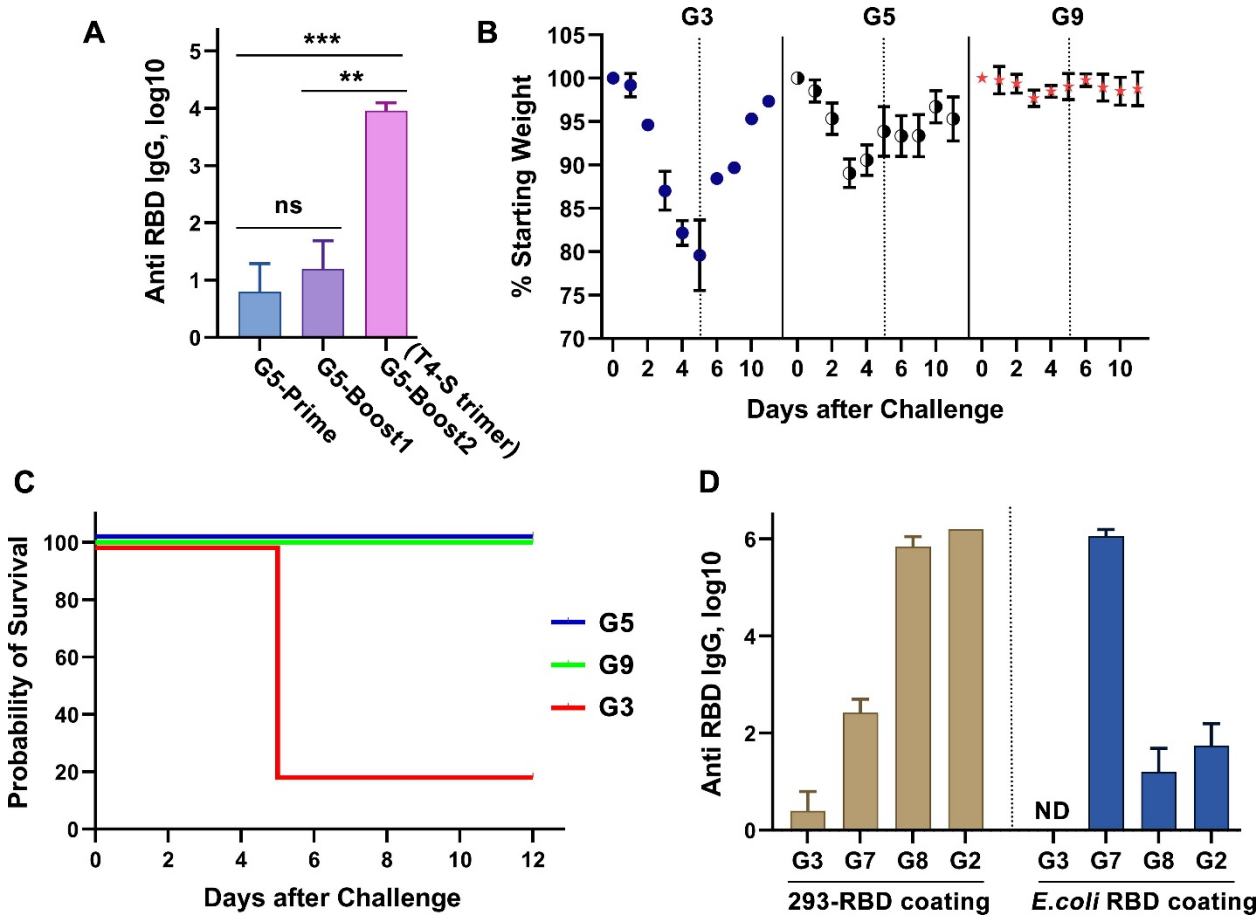

Figure S10. Immune responses of T4-SARS-CoV-2 immunized mice. (**A**) Anti-RBD IgG antibody titers in the sera from group G5 (T4-HocΔ-SocΔ-S-ecto-Ee-NP) at weeks 2 (prime), 5 (boost-1), and 8 (boost-2). For boost-2, T4-S-trimers particles were used. **P < 0.01 and ***P < 0.001. (**B**) Body weight of immunized mice from groups G3 (phage control), G5 (T4-S DNA plus T4-S-trimers boost-2), and G9 (T4-S-trimers) at days post-challenge with 10^5 pfu of SARS-CoV-2 MA10 virus (intranasal inoculation). (**C**) Survival rate of groups G3, G5, and G9 after virus challenge. (**D**) Comparison of anti-RBD IgG antibody titers by ELISA using HEK293-produced RBD or *E. coli*-produced RBD as coating antigens in groups G3 (phage control), G7 (rRBD displayed T4), G8 (T4-S-trimers), and G2 (S-trimers-Alhydrogel).

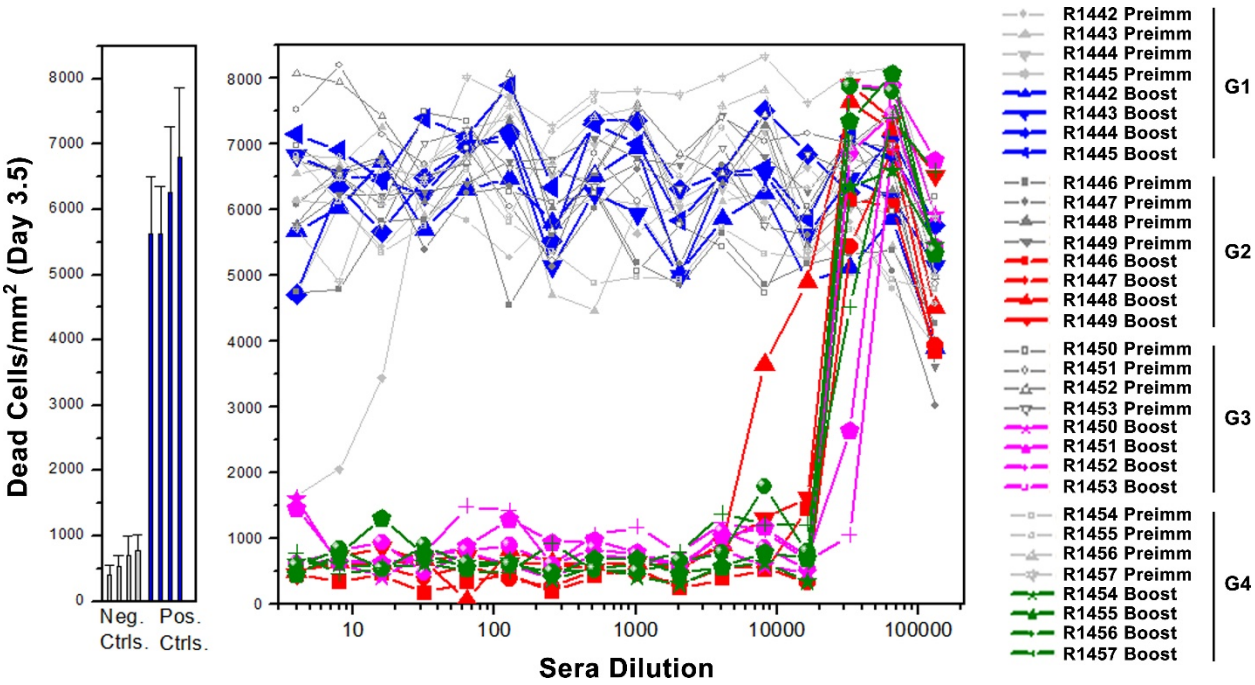

Figure S11. Virus neutralization titers of rabbit sera. Infection of Vero E6 cells by live SARS-CoV-2 US-WA-1/2020 was determined in the presence of rabbit sera at a series of two-fold dilutions starting from 1:4. Culture medium only and CoV-2 virus only were used as negative and positive controls, respectively. R1442 to R1457 refer to tag numbers of rabbits. The data in control groups were presented as means ± SD of 32 wells. The data in rabbit sera groups were shown as means of duplicates.

Table S1. Cpf1/Cas9 spacer information used in this study.

Spacers	Sequence (5'-3')	GC, %	
Cpf1-39-56-sp1	gttgcattaatcagcatcag	40	39-56 11 Kbp deletion
Cpf1-39-56-sp2	cgcccttgaagttccttctg	55	
Cpf1-FarP7K-sp1	tccactccaagatgctccat	50	FarP 7 Kbp deletion; CAG-CD5-Sfl or CAG-CD5-S-ecto insertion
Cpf1-FarP7K-sp2	aaaccgttcaagagtttttg	35	
Cpf1-FarP7K-sp3	aatttagcactcgtggagat	40	
Cpf1-FarP7K-sp4	tcgcccgaatgaatccagtt	50	
Cpf1-FarP7K-sp5	ggaagaatccgttaatcgtc	45	
Cpf1-FarP7K-sp6	ccagtgagttttcacacgaa	45	
Cpf1-FarP18K-sp1	cactgatgaagaaacggtgt	45	FarP 18 Kbp deletion;
Cpf1-FarP18K-sp2	tctactgtaatcatgtccca	40	
Cpf1-FarP18K-sp3	tcgttggttcattatacacc	40	
Cpf1-FarP18K-sp4	gaattaatcgtgctgataca	35	
Cpf1-SegF-sp1:	ttccttctccaccctgacca	55	SegF deletion, CMV-RBD insertion
Cpf1-SegF-sp2:	atgcagatattagctcacgt	40	
Cpf1-SegF-sp3:	accatcgtattttataatta	20	
Cpf1-Hoc-sp1:	cagttgatataactcctaaa	30	Hoc deletion, Ee or Ec insertion
Cpf1-Hoc-sp2:	atcaataacccctgtaggtg	45	
Cpf1-Hoc-sp3:	gttatgtactaaaaggacct	35	
Cpf1-Hoc-sp4:	gaaactggtatcatctatac	35	
Cpf1-Soc-sp1:	agcagaaattagatggaaat	30	Soc deletion
Cpf1-Soc-sp2:	atattaacataaccgcgagt	35	
Cpf1-Soc-sp3:	cagcaatccattcagtacgt	45	
Cpf1-Soc-sp4:	tggaaagtaactggttaata	30	
Cpf1-Mrh2-sp1:	ttcattacatgtcgtgaaat	30	SpyCatcher or RBD insertion
Cpf1-Mrh2-sp2:	gatattatcatttcacgaca	30	
Cpf1-Mrh2-sp3:	aattcgacttgcttctcacc	45	
Cpf1-IPIII-sp1:	aagtcggaagcctttgtagc	50	IPIII deletion; NP insertion
Cpf1-IPIII-sp2:	tgcttggcaaattcaagacc	45	
Cpf1-IPIII-sp3:	ctgatcggtaggtccactca	55	
Cpf1-IPIII-sp4:	ctacagaagcttcggcaata	45	
Cpf1-IPII-sp1:	cttctaagttcggcatgtct	45	IPII deletion
Cpf1-IPII-sp2:	ttacggtctttatcgggcaa	45	
Cas9-IPIII-sp1:	atggaaaggtcttgatgcaa	40	IPIII deletion; NP insertion
Cas9-IPIII-sp2:	attatcaatgacccatttac	30	
Cas9-IPIII-sp3:	ggcctttactacagaagctt	45	

Supplemental Video. Design of SARS-CoV-2 vaccine by CRISPR engineering of bacteriophage T4.